Journal of Hydraulic Research

Publication details, including instructions for authors and subscription information:
http://www.tandfonline.com/loi/tjhr20

Experimental method for the evaluation of the dynamic transfer matrix using pressure transducers

Keita Yamamoto[a], Andres Müller[b], Takuya Ashida[c], Koichi Yonezawa[d], François Avellan[e] & Yoshinobu Tsujimoto[f]

[a] PhD Student, Laboratory for Hydraulic Machines, École Polytechnique Fédérale de Lausanne, Lausanne, Switzerland

[b] Research Associate, Laboratory for Hydraulic Machines, École Polytechnique Fédérale de Lausanne, Lausanne, Switzerland Email:

[c] Master Student, Graduate School of Engineering Science, Osaka University, Osaka, Japan Email:

[d] Assistant Professor, Graduate School of Engineering Science, Osaka University, Osaka, Japan Email:

[e] (IAHR Member), Professor, Laboratory for Hydraulic Machines, École Polytechnique Fédérale de Lausanne, Lausanne, Switzerland Email:

[f] Professor, Osaka University, Graduate School of Engineering Science, Osaka, Japan Email:

Published online: 15 Jul 2015.

To cite this article: Keita Yamamoto, Andres Müller, Takuya Ashida, Koichi Yonezawa, François Avellan & Yoshinobu Tsujimoto (2015): Experimental method for the evaluation of the dynamic transfer matrix using pressure transducers, Journal of Hydraulic Research, DOI: 10.1080/00221686.2015.1050076

To link to this article: http://dx.doi.org/10.1080/00221686.2015.1050076

Journal of Hydraulic Research, 2015
http://dx.doi.org/10.1080/00221686.2015.1050076

Research paper

Experimental method for the evaluation of the dynamic transfer matrix using pressure transducers

KEITA YAMAMOTO, PhD Student, *Laboratory for Hydraulic Machines, École Polytechnique Fédérale de Lausanne, Lausanne, Switzerland*
Email: keita.yamamoto@epfl.ch (author for correspondence)

ANDRES MÜLLER, Research Associate, *Laboratory for Hydraulic Machines, École Polytechnique Fédérale de Lausanne, Lausanne, Switzerland*
Email: andres.mueller@epfl.ch

TAKUYA ASHIDA, Master Student, *Graduate School of Engineering Science, Osaka University, Osaka, Japan*
Email: takuya.ashida@flow.me.es.osaka-u.ac.jp

KOICHI YONEZAWA, Assistant Professor, *Graduate School of Engineering Science, Osaka University, Osaka, Japan*
Email: yonezawa@me.es.osaka-u.ac.jp

FRANÇOIS AVELLAN (IAHR Member), Professor, *Laboratory for Hydraulic Machines, École Polytechnique Fédérale de Lausanne, Lausanne, Switzerland*
Email: francois.avellan@epfl.ch

YOSHINOBU TSUJIMOTO, Professor, *Osaka University, Graduate School of Engineering Science, Osaka, Japan*
Email: tujimoto@me.es.osaka-u.ac.jp

ABSTRACT
This paper introduces an experimental method for the evaluation of dynamic transfer matrices using only pressure transducers. The discharge fluctuations are evaluated from the fluctuation of the pressure difference at different streamwise locations. The transfer matrices of the resistance, the inertance and the compliance elements are determined by using simple flow configurations. This method is then validated by comparing the transfer matrix components to theoretical values. The results show that the direct measurement of the transfer matrices produces good results below the first structural eigenfrequency of the system. Furthermore, a deviation from the mass continuity in the amplitude ratio of the fluctuating upstream and downstream discharges is investigated. This behaviour can be explained with a simple model taking into account the compliance in the system.

Keywords: Dynamic transfer matrix; experimental facilities; hydraulic machines; one-dimensional models; oscillatory flows; velocity measurements

1 Introduction

The transfer matrix approach is commonly used to characterize and investigate various types of dynamical flow behaviour in hydraulic systems. In a global one-dimensional model, the transfer matrix relates the state quantities of pressure and discharge. The main parameters derived from this transfer matrix are the resistance, inertance, and compliance for cavitation-free conditions as well as the mass flow gain factor and cavitation compliance in the presence of cavitation (Brennen & Acosta, 1976; Chaudhry, 2014; Rubin, 2004; Stirnemann, Eberl, Bolleter, & Pace, 1987). Some of these parameters play a decisive role in the prediction of the unstable behaviour in a flow system. By an analytical approach, Tsujimoto, Kamijo, & Brennen (2001) showed that for the case of cavitating pump systems a normal surge is caused by

Received 15 November 2013; accepted 7 May 2015/Currently open for discussion.

ISSN 0022-1686 print/ISSN 1814-2079 online
http://www.tandfonline.com

a "negative" resistance corresponding to a positive slope of the pump pressure-discharge characteristics. The same authors demonstrated that a cavitation surge is induced by a positive mass flow gain factor, representing the cavity volume increase caused by the upstream discharge decrease of the pump. In the context of hydraulic turbines, the mass flow gain factor and cavitation compliance are used for the stability analyses by Koutnik & Pulpitel (1996), Chen et al. (2008) and Alligné, Nicolet, Tsujimoto, & Avellan (2014). The corresponding instabilities involve complex unsteady flow fields in the draft tube with significant discharge fluctuations, as recently reported by Müller, Dreyer, Andreini, & Avellan (2013). Thus, for the discussion of the hydraulic system stability, it is essential to establish a reliable method to measure the transfer matrix. Brennen & Acosta (1976) evaluated the transfer matrix of a cavitating inducer using a quasi-steady calculation of the blade surface cavitation. The first reliable experimental data were obtained by Ng & Brennen (1978) and Brennen, Meissner, Lo, & Hoffman (1982). They initially used Laser Doppler Velocimetry (LDV) for measuring the fluctuating discharge to compute the transfer matrix, and later an electromagnetic flow meter as a supplementary tool. Rubin (2004) re-examined the data given by Brennen et al. (1982) to obtain a better correlation. Stirnemann et al. (1987) investigated the transfer matrices of a pump by using a pressure transfer function and admittance to avoid the fluctuating discharge measurement. They also developed the electrical network model for the dynamic behaviour of pumps by the extracted parameters from the transfer matrix. Carta, Charley, & Caignaert (2000) examined the transfer matrices of single volute centrifugal pumps from 20 Hz up to 150 Hz and found that the transfer matrix is not largely affected by the operating conditions. In the case of hydraulic turbines, Jacob, Prénat, & Maria (1988) and Jacob & Prénat (1991) proposed the transfer matrix method for the evaluation of the dynamic transmission characteristics of hydraulic machines. This method was also applied by Doerfler (1982) in order to model the pressure surge and the global transmission of the pressure at part load conditions in a Francis turbine by using a transfer matrix model. Philibert & Couston (1998) evaluated the transfer matrix of the cavitation vortex rope at part load condition. The use of dynamic transfer matrices are also successfully applied to the leakage detection in complex pipeline systems with the frequency-response function method, as described by Duan, Lee, Ghidaoui, & Tung (2011).

However, a proper evaluation of transfer matrices requires the accurate measurement of the fluctuating discharge. Even if electromagnetic flow meters are suitable tools for this purpose, they require to be calibrated by other available methods. The aim of the present study is to investigate if the measurements of transfer matrices can be performed with pressure transducers only. In other words, if the discharge fluctuations can be accurately evaluated from the pressure difference at two different streamwise locations by extending the pressure-time method, introduced by Gibson (1923) and described in the IEC 60041 standard (1999), to fluctuating flows. Washio, Takahashi, & Yamaguchi (1996) and Washio, Takahashi, Yu, & Yamaguchi (1996) examined the characteristics of the unsteady orifice flow in an oil hydraulic line by using the discharge fluctuations measured by two individual pressure sensors. In the same way, Dazin, Caignaert, & Bois (2007) investigated the transient behaviour of a radial pump during a fast start-up. They confirmed the validity of this fluctuating discharge measurement method by comparison with an electromagnetic flow meter. Kashima, Lee, Ghidaoui, & Davidson (2013) evaluated the accuracy of this method using the simple pipe line, and succeeded in measuring the unsteady discharge by this method with acceptable accuracy under laminar and turbulent flow conditions.

The study presented in this paper validates the direct measurement method of the transfer matrix with pressure transducers through a systematic application to simple flow configurations with resistance, inertance and compliance elements (Fig. 6, later). The accuracy of the results is confirmed by comparison with theoretical values evaluated from the estimated resistance, inertance and compliance.

Finally, in spite of satisfying results obtained by the use of the transfer matrices in past studies, an issue concerning the mass continuity condition is reported by Rubin (2004) for the case of cavitation-free flow in an inducer. This issue is resolved in the present work by the systematic evaluation of the transfer matrices and the corresponding discharge ratios for the different flow configurations. The comparison with the result from a simple analytical model shows that the discharge ratio is influenced by the compliance in the system.

2 Transfer matrix

The equations used to obtain the following transfer matrix components are based on the one-dimensional (1D) representation of transient flows, which are described by, among others, Streeter & Wylie (1967) or more recently in a review by Ghidaoui, Zhao, McInnis, & Axworthy (2005). In the present study, the following assumptions are made.

- The flow in the straight, circular pipes of the test rig is considered to be one-dimensional, inviscid and incompressible.
- The pressure p and the discharge Q are decomposed into steady and fluctuating components, and are represented by $p = \bar{p} + \tilde{p}$, $Q = \bar{Q} + \tilde{Q}$ (- : steady component, $\sim$: fluctuation component). The amplitude of the fluctuation components is assumed to be sufficiently small compared with a steady part ($|\tilde{p}| \ll \bar{p}$, $|\tilde{Q}| \ll \bar{Q}$). Hence, the equations can be linearized. This hypothesis is supported by comparing the amplitude of the induced discharge fluctuations to the mean value measured in the test rig. The amplitude of the discharge fluctuation was adjusted to be less than 2% of the mean discharge, for instance 3.33×10^{-5} m^3 s^{-1} (1.3% of the mean discharge) at 2 Hz, and 0.95×10^{-5} m^3 s^{-1} (0.4% of the

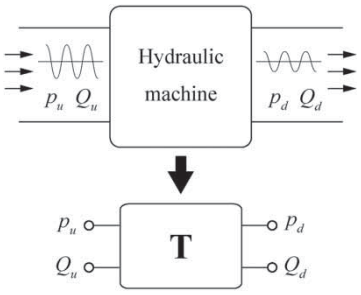

Figure 1 Model of a transfer matrix

mean discharge) at 20 Hz with the downstream exciter. The amplitude of the discharge fluctuations with the upstream exciter was adjusted to produce the same level as with the downstream excitation.

- All the elements of fluctuating pressure $\tilde{p}$ and discharge $\tilde{Q}$ oscillate with a time dependence of $\exp(j\omega t)$ where $\omega = 2\pi f$ is the angular frequency and j is the imaginary unit. The fluctuation components of the pressure and discharge are written as:

$$\tilde{p} = p_f \exp(j\,\omega t) \tag{1}$$

$$\tilde{Q} = Q_f \exp(j\,\omega t) \tag{2}$$

Then, the relationship between the state variables at both sides of a hydraulic system component can be expressed by the transfer matrix **T** (Fig. 1) which yields (Brennen & Acosta, 1976; Carta et al., 2000; Rubin, 2004; Stirnemann et al., 1987)

$$\begin{pmatrix} \tilde{p}_d \\ \tilde{Q}_d \end{pmatrix} = \mathbf{T} \begin{pmatrix} \tilde{p}_u \\ \tilde{Q}_u \end{pmatrix} = \begin{pmatrix} T_{11} & T_{12} \\ T_{21} & T_{22} \end{pmatrix} \begin{pmatrix} \tilde{p}_u \\ \tilde{Q}_u \end{pmatrix} \tag{3}$$

where $\tilde{p}_u$ and $\tilde{Q}_u$ represent the upstream (suffix u) pressure and discharge fluctuations and $\tilde{p}_d$ and $\tilde{Q}_d$ are the corresponding downstream (suffix d) quantities. The elements of the transfer matrices for the following simple flow components are theoretically evaluated, as described by several authors in the past (Brennen, 1994; Chaudhry, 2014).

2.1 *Transfer matrix of a resistance*

If we assume a resistance with a negligible length, such as an orifice (see Fig. 2), the pressure difference is expressed by the resistance coefficient and the flow velocity. Focusing on the fluctuating components, we can derive the following equation

$$\tilde{p}_d - \tilde{p}_u = -\zeta \frac{\bar{Q}}{A^2} \tilde{Q}_u \tag{4}$$

where ζ represents the resistance coefficient, A is the pipe cross-section area and $\bar{Q} = \bar{Q}_u = \bar{Q}_d$.

The equation of continuity can be written as

$$\tilde{Q}_d - \tilde{Q}_u = 0 \tag{5}$$

From Eqs. (4) and (5), the transfer matrix of a pure resistance can be expressed as follows

$$\begin{pmatrix} \tilde{p}_d \\ \tilde{Q}_d \end{pmatrix} = \begin{pmatrix} 1 & -\zeta \frac{1}{A^2} \bar{Q} \\ 0 & 1 \end{pmatrix} \begin{pmatrix} \tilde{p}_u \\ \tilde{Q}_u \end{pmatrix} = \begin{pmatrix} 1 & -R \\ 0 & 1 \end{pmatrix} \begin{pmatrix} \tilde{p}_u \\ \tilde{Q}_u \end{pmatrix} \tag{6}$$

2.2 *Transfer matrix of an inertance*

In the case of a frictionless pipe with a length l (see Fig. 3), the pressure difference can be expressed by the inertia of the fluctuating discharge. Considering Eqs. (1) and (2), this difference is written as

$$\tilde{p}_d - \tilde{p}_u = -j\,\omega \frac{\rho l}{A} \tilde{Q}_u \tag{7}$$

where ρ is the density. Combining Eqs. (5) and (7), we can derive the transfer matrix of a pure inertance

$$\begin{pmatrix} \tilde{p}_d \\ \tilde{Q}_d \end{pmatrix} = \begin{pmatrix} 1 & -j\,\omega \frac{\rho l}{A} \\ 0 & 1 \end{pmatrix} \begin{pmatrix} \tilde{p}_u \\ \tilde{Q}_u \end{pmatrix} = \begin{pmatrix} 1 & -j\,\omega L \\ 0 & 1 \end{pmatrix} \begin{pmatrix} \tilde{p}_u \\ \tilde{Q}_u \end{pmatrix} \tag{8}$$

2.3 *Transfer matrix of a compliance*

If a pipe is elastic or contains trapped air (Fig. 4), the equation of continuity can be expressed as:

$$\tilde{Q}_d - \tilde{Q}_u = \frac{\mathrm{d}V_{air}}{\mathrm{d}t} - \frac{\mathrm{d}V_{pipe}}{\mathrm{d}t} = \frac{\mathrm{d}V_c}{\mathrm{d}t} \tag{9}$$

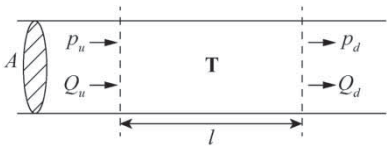

Figure 3 Model of a transfer matrix of inertance

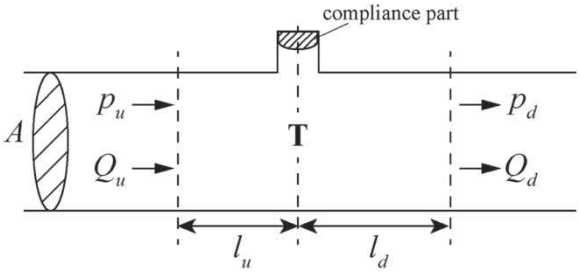

Figure 4 Model of a transfer matrix of compliance

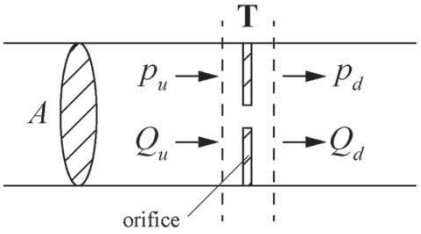

Figure 2 Model of a transfer matrix of resistance

where V_{air} and V_{pipe} are the trapped air and pipe volumes, and $V_c = V_{air} - V_{pipe}$. The compliance C is defined by

$$C = \frac{\mathrm{d}V_c}{\mathrm{d}p_u} \tag{10}$$

Combining Eqs. (1), (9) and (10), the following equation for the discharge difference can be derived as

$$\tilde{Q}_d - \tilde{Q}_u = \frac{\mathrm{d}V_c}{\mathrm{d}p_u}\frac{\mathrm{d}p_u}{\mathrm{d}t} = j\omega C\tilde{p}_u \tag{11}$$

If we separately take into account the inertance placed in the upstream and downstream of the compliance (l_u and l_d in Fig. 4), the pressure difference is written in the form

$$\tilde{p}_d - \tilde{p}_u = -\frac{\rho l_u}{A}\frac{\mathrm{d}\tilde{Q}_u}{\mathrm{d}t} - \frac{\rho l_d}{A}\frac{\mathrm{d}\tilde{Q}_d}{\mathrm{d}t} = -j\omega L_u\tilde{Q}_u - j\omega L_d\tilde{Q}_d \tag{12}$$

Thus, we can derive the transfer matrix of a compliance from Eqs. (11) and (12)

$$\begin{pmatrix}\tilde{p}_d\\ \tilde{Q}_d\end{pmatrix} = \begin{pmatrix}1+\omega^2 CL_d & -j\omega L_u - j\omega L_d\\ j\omega C & 1\end{pmatrix}\begin{pmatrix}\tilde{p}_u\\ \tilde{Q}_u\end{pmatrix} = \begin{pmatrix}1+\omega^2 CL_d & -j\omega L\\ j\omega C & 1\end{pmatrix}\begin{pmatrix}\tilde{p}_u\\ \tilde{Q}_u\end{pmatrix} \tag{13}$$

where $L = L_u + L_d$.

In order to validate the method for evaluating transfer matrices, simple experimental arrangements are prepared (Fig. 6). The transfer matrices of the resistance and inertance were examined with the straight pipe configuration (see Fig. 6a), and the matrix of the compliance with the T-pipe configuration which has a branch pipe to trap air (Fig. 6b).

Equation (3) suggests that two independent sets of oscillation modes are required in order to determine the four elements of the transfer matrix (Brennen & Acosta, 1976; Carta et al., 2000; Rubin, 2004; Stirnemann et al., 1987). Therefore, two exciters (upstream and downstream exciters) are installed (Fig. 6).

3 Measurement of discharge fluctuation

Based on the axial momentum balance for a one-dimensional inviscid flow, the relationship between a pressure difference of two arbitrary points and a discharge in the pipe with a constant cross-section area A can be written by the following equation

$$p_{\mathrm{I}} - p_{\mathrm{II}} = \frac{\rho l}{A}\frac{\mathrm{d}Q}{\mathrm{d}t} \tag{14}$$

where l is the length between the two pressure locations p_{I} and p_{II}. Then, the discharge fluctuation can be computed from Eq. (14). The discharge fluctuation becomes

$$\tilde{Q} = \frac{A}{\rho l}\int (p_{\mathrm{I}} - p_{\mathrm{II}})\mathrm{d}t \tag{15}$$

In the present study, the upstream and the downstream discharge fluctuations are calculated using $\tilde{p}_A = \tilde{p}_B$ and $\tilde{p}_C - \tilde{p}_D$ respectively (see Section 4), as in

$$\tilde{Q}_u = \frac{A}{\rho l_{AB}}\int (\tilde{p}_A - \tilde{p}_B)\mathrm{d}t \tag{16}$$

$$\tilde{Q}_d = \frac{A}{\rho l_{CD}}\int (\tilde{p}_C - \tilde{p}_D)\mathrm{d}t \tag{17}$$

where l_{AB} and l_{CD} are the distances between p_A and p_B and between p_C and p_D, respectively (Fig. 6).

In the time domain, the integrals in Eqs. (16) and (17) are evaluated by Simpson's rule, thus the nth component of the discharge fluctuation is written as follows

$$\tilde{Q}_{u,n} = \frac{A}{\rho l_{AB}}\frac{\Delta t}{3}[(\tilde{p}_A - \tilde{p}_B)_{n+1} + 4(\tilde{p}_A - \tilde{p}_B)_n + (\tilde{p}_A - \tilde{p}_B)_{n-1}] + \tilde{Q}_{u,n-2} \tag{18}$$

$$\tilde{Q}_{d,n} = \frac{A}{\rho l_{CD}}\frac{\Delta t}{3}[(\tilde{p}_C - \tilde{p}_D)_{n+1} + 4(\tilde{p}_C - \tilde{p}_D)_n + (\tilde{p}_C - \tilde{p}_D)_{n-1}] + \tilde{Q}_{d,n-2} \tag{19}$$

where $\Delta t = 1/fs = 0.001$ s. As an example, the time history of the pressure and discharge fluctuations evaluated from Eqs. (18) and (19) at 2 Hz excitation with the upstream and downstream exciters are shown in Fig. 5. In both cases of upstream and downstream excitation, the pressure and discharge traces have a sinusoidal oscillation. A small pulsation with a period of about 0.05 s is observed in the pressure traces. However, this component is more or less cancelled in the process of subtraction

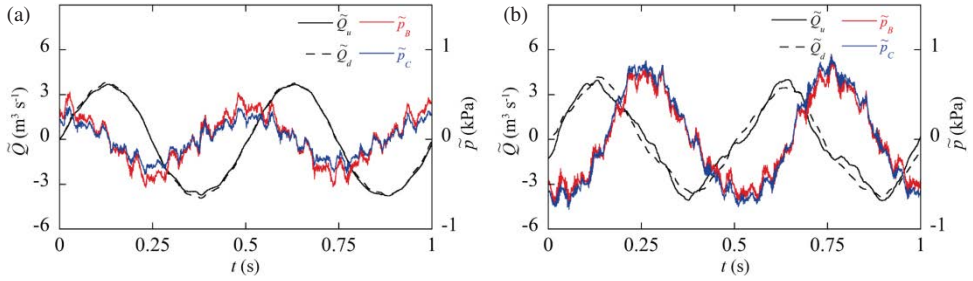

Figure 5 Two cycles time history of the discharge and pressure fluctuations with the upstream exciter (a) and the downstream exciter (b), both operated at 2 Hz

($\tilde{p}_A - \tilde{p}_B$ and $\tilde{p}_C - \tilde{p}_D$), therefore it does not appear in the discharge traces. As mentioned above, the two linearly independent oscillation modes are required to determine the four elements of the transfer matrix **T**. We can observe that both upstream and downstream discharges oscillate with the phase delay of $\pi/2$ behind the pressure waves with the upstream exciter (Fig. 5a). On the other hand, the pressure waves precede the discharges by $\pi/2$ with the downstream exciter (Fig. 5b). This suggests that the independent excitation mode is obtained by using the upstream and downstream exciters.

In the frequency analysis for computing the transfer matrix, upstream and downstream discharge fluctuations are calculated as follows using Eqs. (1) and (2)

$$\tilde{Q}_u = \frac{A}{\rho l_{AB}} \frac{\tilde{p}_A - \tilde{p}_B}{j\omega} \tag{20}$$

$$\tilde{Q}_d = \frac{A}{\rho l_{CD}} \frac{\tilde{p}_C - \tilde{p}_D}{j\omega} \tag{21}$$

4 Experimental set up

The sketch of the experimental facility with the straight pipe to evaluate the transfer matrix of resistance and inertance is shown in Fig. 6a. It includes four pressure transducers (p_A, p_B, p_C and p_D), a downstream tank, an electromagnetic flow meter, a centrifugal pump and flow exciters upstream and downstream of the four pressure transducers. The accuracy of the unsteady discharge measurement is heavily dependent on an accurate measurement for the pressure difference. The pressure transducers are of differential type with a range of 0 kPa to 10 kPa and an accuracy of 4 Pa (GE sensing, UNIK5000 PMP5078, manufacturer calibrated). All the transducers used for the measurements have the same characteristics. The upstream and downstream pipes with the pressure transducers are made of acrylic resin and the distances between p_A and p_B, and between p_C and p_D are 0.82 m for both cases. The upstream and downstream flow exciters generating sinusoidal and one-dimensional flow fluctuations use piston and rotary valves, respectively. The mean discharge is adjusted by the pump speed. In the present study, the mean discharge value is set constant at 2.5×10^{-3} m^3 s^{-1}. In order to add the resistance between p_B and p_C sections, two types of orifice plates were installed in the middle of the straight pipe (conditions 2, 3 in Table 1). The diameter ratios of the orifices A and B are $d/D = 0.42$ and $d/D = 0.32$ respectively, where d represents the orifice aperture diameter, and D the pipe inner diameter. The thickness of the orifice plates is 4 mm. The inertance value is varied by changing the pipe length between p_B and p_C (condition 4 in Table 1).

The T-pipe configuration to evaluate the transfer matrix of a compliance is shown in Fig. 6b. The length between p_B and p_C is the same as for the straight pipe configuration. This T-pipe part is made of PVC pipes. Air is introduced from the valve on the top of the branch pipe and its volume is varied to change the compliance between p_B and p_C. The amount of air is adjusted to 0 ml (no air), 4 ml and 8 ml (conditions 5, 6, and 7 in Table 1). The excitation frequency is varied from 1 Hz through 30 Hz every 1 Hz. The pipe properties and the experimental conditions in this study are summarized in Tables 1 and 2 respectively. All

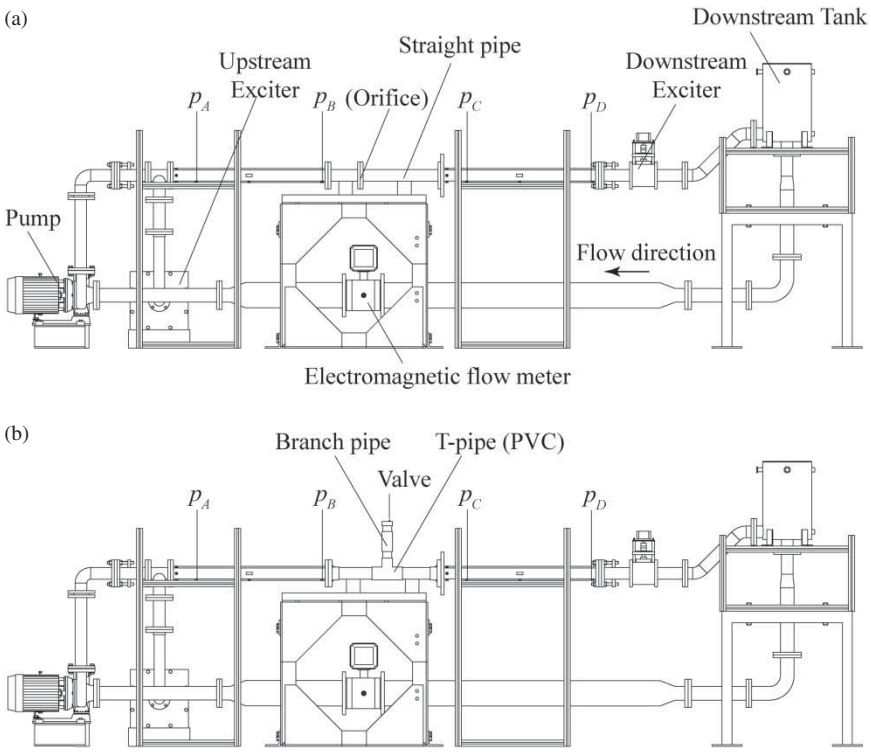

Figure 6 Straight pipe configuration (a) and T-pipe configuration (b)

measurements were carried out with a sampling frequency $fs = 1000$ Hz.

In the present study, p_B and p_C are respectively used as the upstream/downstream pressure fluctuations p_u and p_d, and the transfer matrices between the locations p_B and p_C are calculated.

Table 1 Properties of pipes

Pipe	Material	Inner diameter (m)	Outer diameter (m)
Upstream and downstream pipes with pressure transducers	Acrylic resin	0.07	0.09
Straight pipe	Stainless steel	0.072	0.076
T-pipe (main pipe)	Poly vinyl chloride resin	0.068	0.076
T-pipe (branch pipe)	Poly vinyl chloride resin	0.052	0.060

Table 2 Experimental conditions

Condition	Resistance	Distance between p_B and p_C (m)	Volume of air (ml)	Configuration
1	-	0.93	0	Straight pipe
2	Orifice A	0.93	0	Straight pipe
3	Orifice B	0.93	0	Straight pipe
4	-	0.41	0	Straight pipe
5	-	0.93	0	T-pipe
6	-	0.93	4	T-pipe
7	-	0.93	8	T-pipe

5 Experimental results

5.1 *Transfer matrix of a resistance and an inertance*

The values of the transfer matrix elements of the resistance and inertance are shown in Figs. 7 and 8. The values of the resistance and the inertance affects only T_{12} as expected from Eqs. (6) and (8). As for T_{11} and T_{22}, good agreements with the theoretical value $1 + 0j$ are obtained for all conditions. In the plot of T_{12}, the quasi-steady resistance $-R_e$ shown by dashed lines is evaluated from the slope of the pressure drop curve shown in Fig. 9. The difference from this value is small even at higher frequencies with both orifices. The inertance L_e is evaluated from the distance between p_B and p_C measurement locations and $-j\omega L_e$ is plotted in the figure. The measured results are in good agreement with the estimated values. Equations (6) and (8) suggest that T_{21} should be zero in the absence of the compliance. However, the imaginary part of T_{21} is likely to decrease in proportion to the frequency in all cases. It implies that even the straight pipe configuration has a small compliance between the measurement locations of p_B and p_C.

The amplitude ratio and the phase difference of the upstream and downstream discharge fluctuations is reported in Fig. 10. It can be observed that the amplitude ratio deviates from the unity as the frequency is increased. The amount of deviation does not depend on the resistance and the inertance. The amplitude ratio is increasing for the case with the upstream exciter and decreasing with the downstream exciter. The phase difference is almost zero in all frequencies with both the upstream and downstream exciters. This is discussed later.

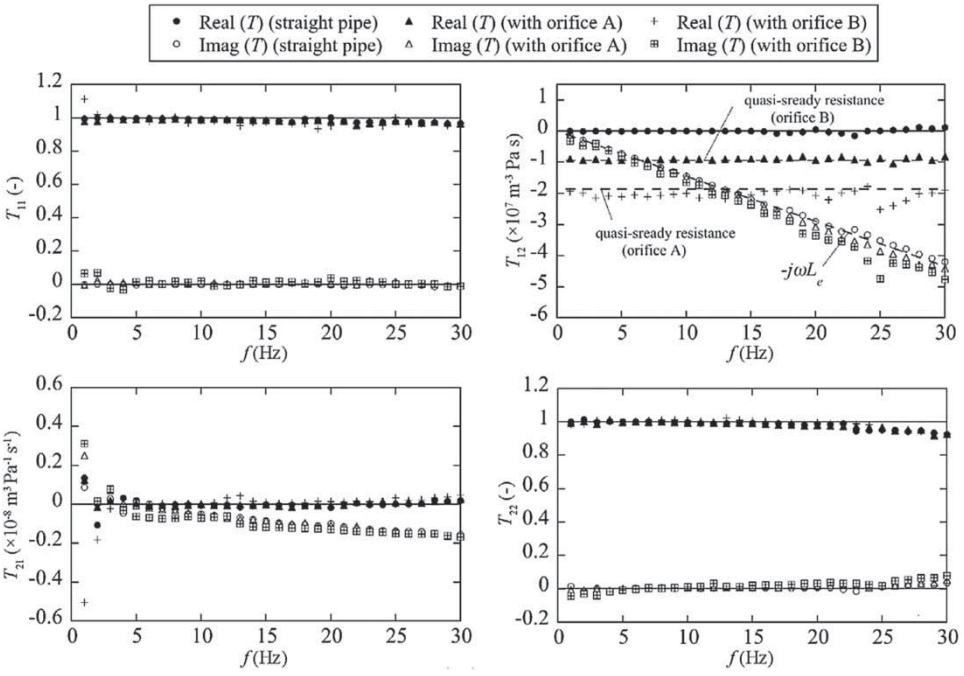

Figure 7 Transfer matrix elements of resistance as a function of frequency f

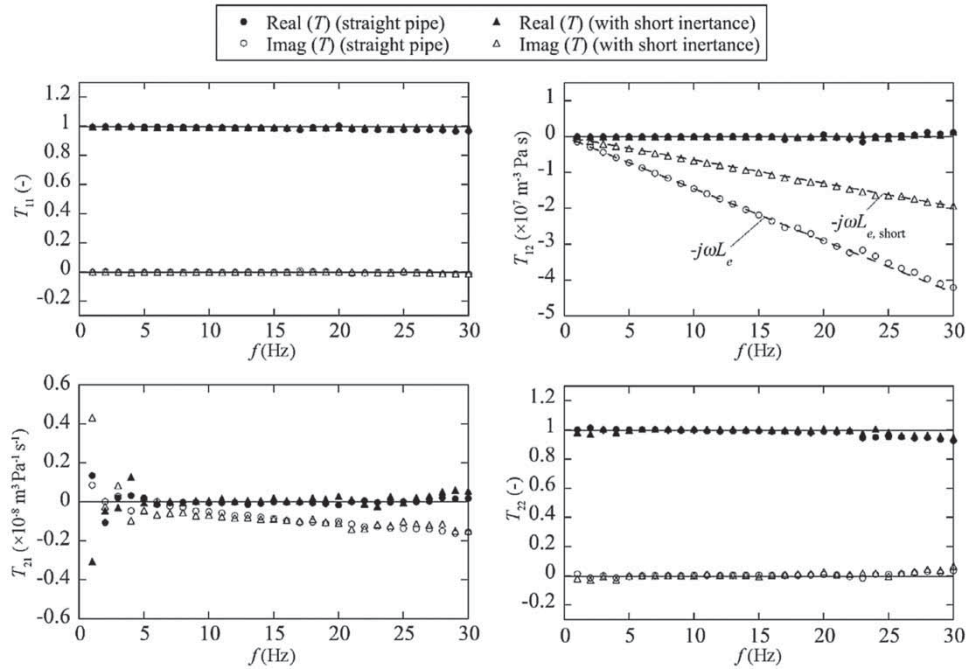

Figure 8 Transfer matrix elements of inertance as a function of the frequency f

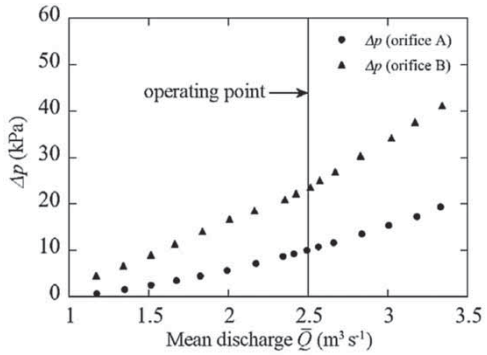

Figure 9 Pressure difference $\Delta p = p_B - p_C$ between the upstream and downstream positions of the orifice A and orifice B

5.2 *Transfer matrix of a compliance*

The comparison of the transfer matrix elements obtained with the T-pipe configuration with various amount of air trapped in the branch pipe is made in Fig. 11. The amount of air mainly affects the value of the T_{21} element. Even with no air in the branch pipe, the imaginary part of T_{21} clearly decreases with an increase of the frequency. This suggests that the PVC pipe itself features a non-negligible compliance. Assuming that the axial strain is zero, the pipe volume increase due to an internal pressure increase can be written as follows:

$$\delta V_{pipe} = \frac{2\pi r^3 l_{pipe}(1-\nu^2)}{t_p E}\delta p \tag{22}$$

where r represents the pipe radius, l_{pipe} is the pipe length, ν is the Poisson ratio, t_p is the thickness of the pipe and E is the Young's modulus. Hence, the compliance due to the change of the pipe volume can be expressed as:

$$C_e = \frac{\mathrm{d}V_{pipe}}{\mathrm{d}p} = \frac{2\pi r^3 l_{pipe}(1-\nu^2)}{t_p E} \tag{23}$$

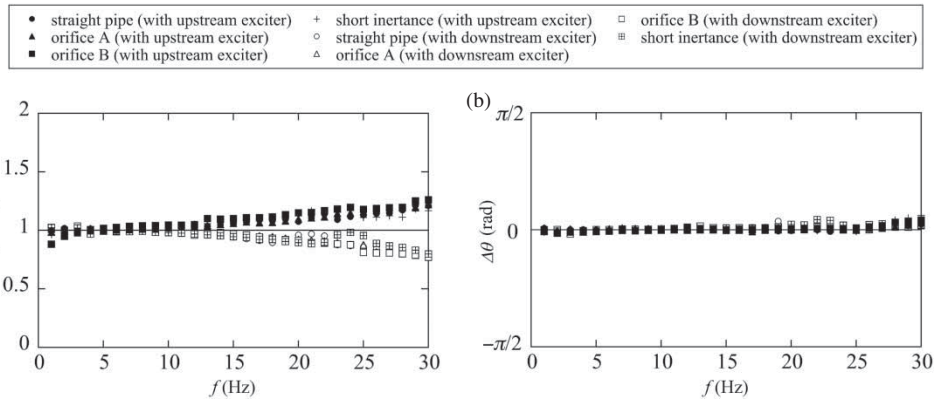

Figure 10 Amplitude ratio $|Q_{f,d}|/|Q_{f,u}|$ (a) and phase difference $\Delta\theta$ (b) of the upstream and downstream discharge fluctuations

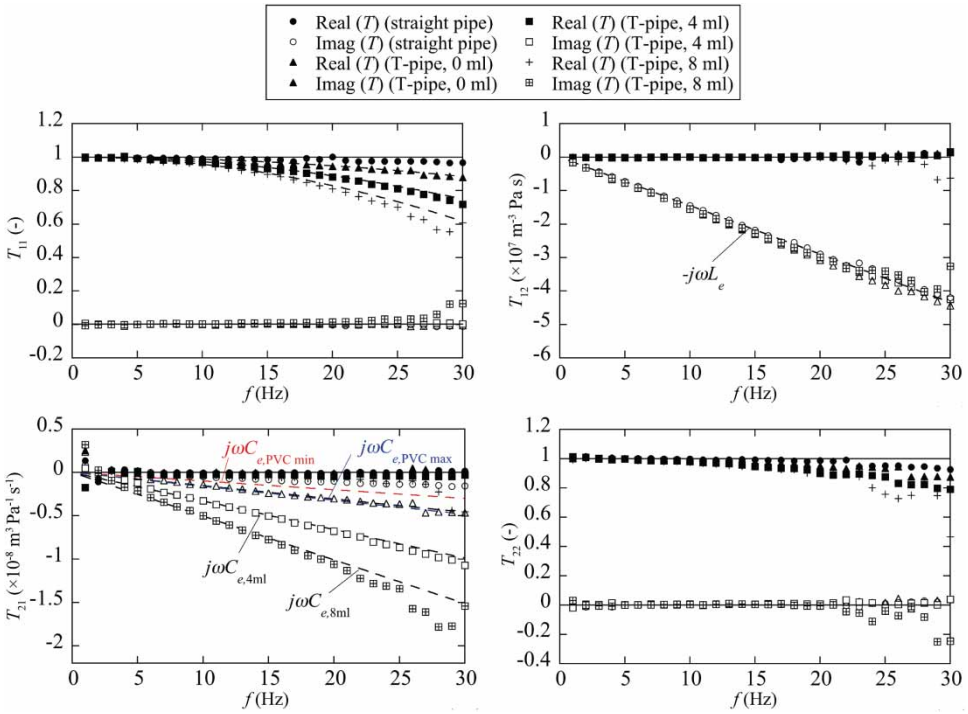

Figure 11 Transfer matrix elements of a compliance as a function of the frequency f

Two slopes of estimated compliance C_e obtained by using the Young's modulus ($E = 2.4$ GPa $\sim E = 4.1$ GPa) of the pipe material PVC are plotted in the figure showing the T_{21} element (Fig. 11). The blue and red dashed lines are slopes ($j\omega C_{e,PVC\,min}$ and $j\omega C_{e,PVC\,max}$) calculated with $E = 2.4$ GPa and $E = 4.1$ GPa, respectively. The absolute value of the measured compliance of the PVC pipe calculated by the least squares method is slightly larger than the maximum of the estimated compliance. Assuming that this compliance originally exists in the PVC pipe, the compliance with 4 ml and 8 ml of air is evaluated from the assumption of an adiabatic transition $pV_{air}{}^{\gamma} = \text{const.}$ and slopes $j\omega C_e$ are plotted as black dashed lines. Reasonable agreements are obtained in both cases. From Eq. (13), the real part of the T_{11} element can be written as $1 + \omega^2 C L_d$ and is plotted in the figure showing T_{11} (see Fig. 11) as black dashed lines. The value of inertance L_d is calculated from the axial length between the centre of the T-pipe and the location of the p_C measurement. The real part of T_{12} showing the resistance $-R$ is almost zero, and the imaginary part of T_{12} showing the inertance $-j\omega L$ is nearly the same as the evaluated value from the distance between the measurement locations of p_B and p_C.

The resistance R, the inertance L and the compliance C obtained by the transfer matrices are shown in Figs. 12a, b, c and d respectively, for all experimental conditions. The theoretical values are also plotted as dashed lines. The agreement of the experimental data with the theoretical values validates the presented transfer matrix method. However, in the cases of the higher resistance and the compliance, a small deviation from the theoretical value is observed at 1 Hz and around 26 Hz. The structural eigenfrequency of the test rig determined from a tapping test is found to be around 26 Hz, and the strong vibrations of the test rig are observed in the transfer matrix measurement test around this frequency. This may induce a complex discharge excitation, which is no longer considered as a one-dimensional perturbation, leading to the error of the experimental data. At 1 Hz, the exciters cannot give a sufficient discharge fluctuation due to the excitation amplitude limitation. This is considered to be the cause of the larger error around 1 Hz.

5.3 *Discharge amplitude ratio and Compliance*

The amplitude ratio and phase difference of the upstream and downstream discharge fluctuations with various values of the compliance are shown in Fig. 13. For the upstream excitation, a significant increase caused by a resonance is observed at 21 Hz with 4 ml and 26 Hz with 8 ml air volumes, respectively. This implies that the deviation of the amplitude ratio from the unity is strongly dependent on the compliance. The phase difference starts to deviate at this resonant frequency, and it finally reaches $-\pi$. For the downstream excitation, the amplitude ratio decreases as the frequency approaches the resonant frequency.

For the case of the upstream excitation, we consider a simplified model as shown in Fig. 14 for the purpose of evaluating the amplitude ratio. If we assume that the pressure in the downstream tank is kept constant, the pressure p at the location of the compliance can be expressed by using the downstream pipe length l_d and the downstream discharge fluctuation $\tilde{Q}_d$, i.e.

$$\tilde{p} = \frac{\rho l_d}{A}\frac{\mathrm{d}\tilde{Q}_d}{\mathrm{d}t} \tag{24}$$

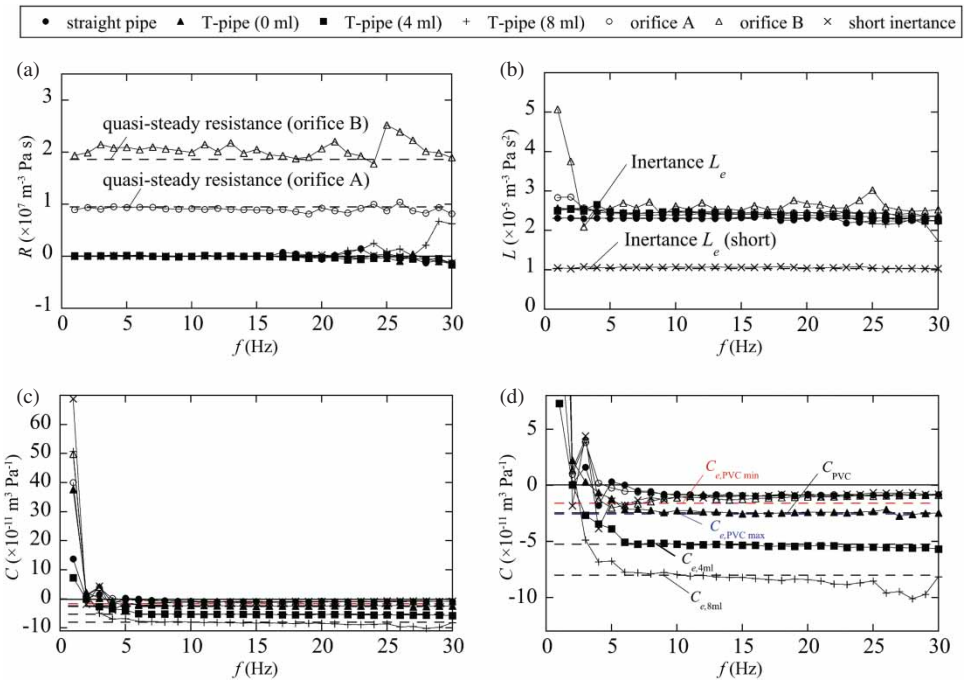

Figure 12 Resistance R (a), inertance L (b), and compliance C (c, d) obtained by the transfer matrix elements

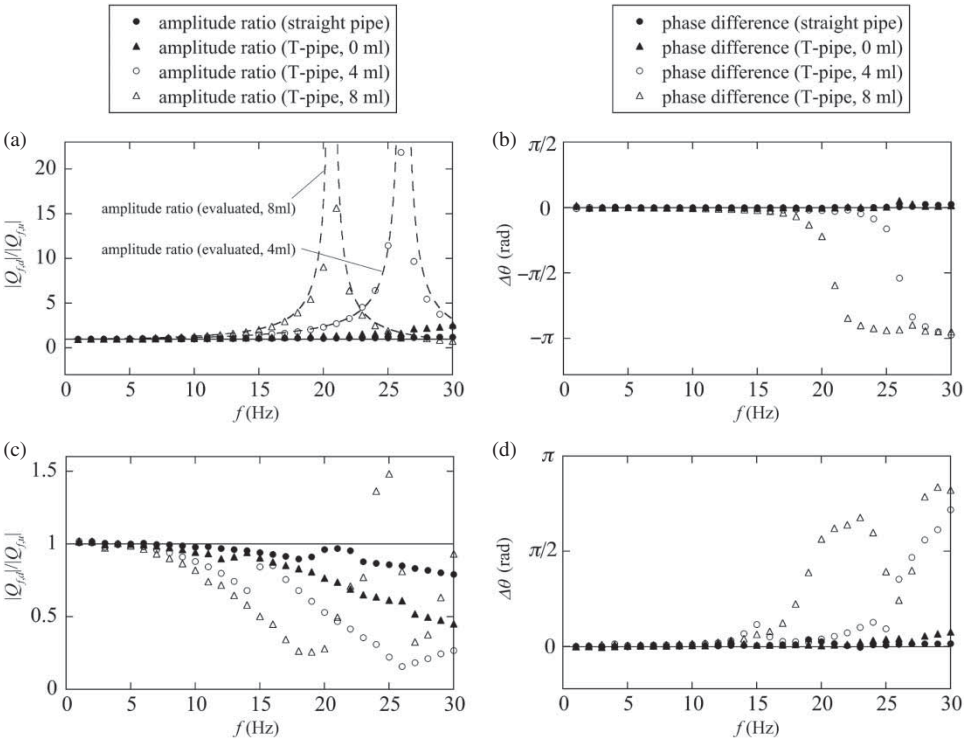

Figure 13 Amplitude ratio $|Q_{f,d}|/|Q_{f,u}|$ and phase difference $\Delta\theta$ of the discharge fluctuations with the upstream exciter (a, b) and the downstream exciter (c, d) and evaluated values of the amplitude ratio by the compliance

The compliance C is defined by the volume of the compliance part V as follows

$$C = \frac{\mathrm{d}V}{\mathrm{d}\tilde{p}} \tag{25}$$

The continuity equation results in:

$$\frac{\mathrm{d}V}{\mathrm{d}t} = j\omega C\tilde{p} = \tilde{Q}_d - \tilde{Q}_u \tag{26}$$

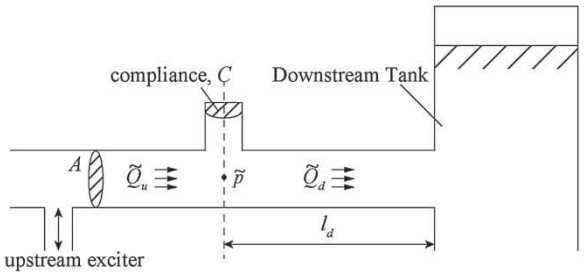

Figure 14 Simplified model of the upstream excitation with a compliance

Hence, the ratio of the upstream and downstream discharge fluctuations can be expressed as:

$$\frac{\tilde{Q}_d}{\tilde{Q}_u} = \frac{1}{1 + \frac{\omega^2 \rho C l_d}{A}} \tag{27}$$

The resonance frequencies estimated by this equation are 20.7 Hz and 26.2 Hz for the cases of 4 ml and 8 ml air volumes, respectively, using the compliance values obtained from the transfer matrix component T_{21} in Fig. 11. The calculated resonance frequencies are close to the values obtained from the experiment results, which are 21 Hz and 26 Hz. The calculated curve from Eq. (27) is plotted in Fig. 13a. Over the resonance frequency, Eq. (27) is calculated assuming that the phase of the upstream and the downstream discharge fluctuations differs by $-\pi$. We can observe that the evaluated curves agree well with the experimental results. Unfortunately, for the downstream excitation the discharge amplitude ratio cannot be evaluated because the upstream boundary condition cannot be easily determined. The amplitude ratio of the upstream and downstream discharge fluctuations also diverges for the cases with the resistance and intertance, although the ratio is much smaller than the cases with the compliance. In Fig. 15, the calculated curve from Eq. (27) is plotted, using the compliance value obtained by the transfer matrices of resistance and inertance in Figs. 7 and 8. Good agreement demonstrates that the deviation from the mass continuity can be described by the compliance evaluated from the transfer matrix element in the straight pipe case.

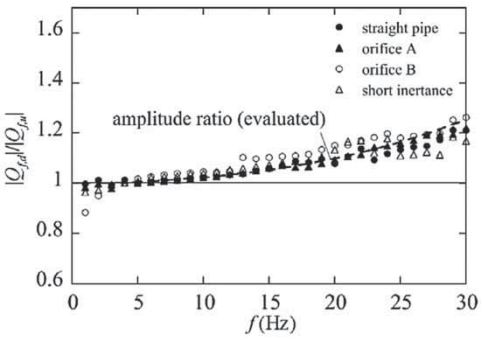

Figure 15 Amplitude ratio $|Q_{f,d}|/|Q_{f,u}|$ obtained from the experimental results and evaluated in the straight pipe configuration

6 Concluding remarks

The presented results show that it is possible to evaluate the dynamic transfer matrix using the discharge fluctuations evaluated from the pressure difference. The agreement of the experimental data with the theoretical values evidences the validity of the aforementioned assumptions of the small discharge perturbation and the one-dimensional flow. However, a small error is induced by the test rig structural eigenfrequency, which in our case is around 26 Hz. At low frequencies around 1 Hz, the error tends to be large due to the insufficient discharge fluctuation. For the flow excitation in this frequency range, it is required to adjust the level of the discharge fluctuation amplitude to ensure the accuracy of measurement, keeping it small enough to be within the range of linear assumption. Except for these frequency ranges, the validity of the transfer matrix method is confirmed by comparing the resistance, inertance and compliance obtained by the transfer matrix elements with the theoretical values evaluated from the estimated resistance, inertance and compliance. We demonstrate that the resonance frequency and the amplitude ratio of the discharge fluctuations are reasonably estimated by a simple calculation model including the compliance in the system. This calculation was also applied to estimate the resonance frequency and the amplitude ratio, and reasonable agreement was obtained. We also showed that the deviation of the amplitude ratio of the discharge fluctuations from 1 in the straight pipe configuration can be explained by the compliance evaluated from the transfer matrix elements.

The successful evaluation of the transfer matrices enables the application of this method to further practical and complex flow systems and hence the proper evaluation of the key dynamic parameters of the systems. The authors are now applying the proposed method to investigate the transfer matrices of an inducer and a hydraulic turbine in order to determine the dynamic characteristics of the cavitation compliance and the mass flow gain factor, which are not well understood yet.

Acknowledgements

The authors would like to acknowledge the contribution of Mr Yuto Motoyama to the successful execution of the experiments.

Disclosure statement

No potential conflict of interest was reported by the authors.

Funding

This research was partially supported by Japan Society for the Promotion of Science (JSPS), Grant in Aid for Young Scientists (B) (grant No.23760158) and by the Turbomachinery Society of Japan, Komiya Research Grant.

Notation

A	=	pipe cross-section area (m^2)
C	=	compliance (m^3 Pa^{-1})
D	=	pipe inner diameter (m)
d	=	aperture diameter of orifice (m)
E	=	Young's modulus (GPa)
f	=	excitation frequency (Hz)
fs	=	sampling frequency (Hz)
j	=	imaginary unit ($j^2 = 1$)
L	=	inertance (m^{-3} Pa s^2)
l	=	length (m)
l_{AB}	=	length between p_A and p_B (m)
l_{CD}	=	length between p_C and p_D (m)
l_{pipe}	=	pipe length (m)
p	=	pressure (Pa)
p_f	=	complex amplitude of pressure (Pa)
Q	=	discharge (m^3 s^{-1})
Q_f	=	complex amplitude of discharge (m^3 s^{-1})
R	=	resistance (m^{-3} Pa s)
r	=	pipe radius (m)
$\mathbf{T}$	=	transfer matrix
t	=	time (s)
T_{ij}	=	transfer matrix element
t_p	=	pipe thickness (m)
V	=	volume (m^3)
V_{air}	=	air volume (m^3)
V_c	=	compliance part volume (m^3)
V_{pipe}	=	pipe volume (m^3)
ν	=	Poisson ratio (–)
θ	=	phase (rad)
ρ	=	density (kg m^{-3})
ω	=	angular frequency (rad s^{-1})
ζ	=	resistance coefficient (m^{-2} Pa s^2)
-	=	steady value
$\sim$	=	fluctuating value
e (suffix)	=	evaluated value
u (suffix)	=	upstream value
d (suffix)	=	downstream value
PVC (suffix)	=	value of PVC pipe

References

Alligné, S., Nicolet, C., Tsujimoto, Y, & Avellan, F. (2014). Cavitation surge modelling in Francis turbine draft tube. *Journal of Hydraulic Research*, *52*, 399–411. doi:10.1080/00221686.2013.854847

Brennen, C. E. (1994). *Hydrodynamics of pumps*. Oxford: Concepts ETI and Oxford University Press.

Brennen, C., & Acosta, A. (1976). The dynamic transfer function for a cavitating inducer. *Journal of Fluid Engineering*, *98*, 182–191.

Brennen, C. E., Meissner C., Lo, E. Y., & Hoffman, G. S. (1982). Scale effects in the dynamic transfer functions for cavitating inducers. *Journal of Fluids Engineering*, *104*, 428–433.

Carta, F., Charley, J., & Caignaert, G. (2000). Transfer matrices of single volute centrifugal pumps. *International Journal of Acoustics and Vibration*, *5*, 159–166

Chaudhry, M. H. (2014). *Applied hydraulic transients* (3rd ed.). New York: Springer.

Chen, C., Nicolet, C., Yonezawa, K., Farhat, M., Avellan, F., & Tsujimoto, Y. (2008). One-dimensional analysis of full load draft tube surge. *Journal of Fluid Engineering*, *130*, 0411061–0411066. doi:10.1115/1.2903475

Dazin, A., Caignaert, G., & Bois, G. (2007). Transient behavior of turbomachineries: applications to radial flow pump startups. *Journal of Fluids Engineering*, *129*, 1436–1444. doi:10.1115/1.2776963

Doerfler, P. (1982). System dynamics of the Francis turbine half load surge. *Proceedings of the 11th IAHR Symposium on Hydraulic Machinery and Systems,* Amsterdam, Netherland, Paper No. 39, 441–453.

Duan, H.-F., Lee, P. J., Ghidaoui, M. S., & Tung, Y.-K. (2011). Leak detection in complex series pipelines by using the system frequency response method. *Journal of Hydraulic Research*, *49*, 213–221. doi:10.1080/00221686.2011.553486

Ghidaoui, M. S., Zhao, M., McInnis, D. A., & Axworthy, D. H. (2005). A review of water hammer theory and practice. *Applied Mechanics Reviews*, *58*, 49–75. doi:10.1115/1.1828050

Gibson, N. R. (1923). The Gibson Method and apparatus for measuring the flow of water in closed conduit. *ASME Power Division*, *45*, 343–392.

IEC 60041. (1999). International standard: field acceptance tests to determine the hydraulic performance of hydraulic turbines, storage pumps and pump-turbines. European Equivalent: EN 60041

Jacob, T., Prénat, J., & Maria, D. (1988). Comportement dynamique d'une turbine Francis à forte charge. Comparaisons modèle-prototype [Dynamic behavior at high load of a Francis water turbine. Model/ prototype comparison]. *La Houille Blanche*, *3*, 293–300.

Jacob, T., & Prénat, J. (1991). Identification of a hydraulic turbomachine's hydro-acoustic transmission parameters. *Proceedings of the IAHR 5th International Meeting of Work Group on the Behaviour of Hydraulic Machinery under Steady Oscillatory Conditions*, Milano, Italy.

Kashima, A., Lee, P. J., Ghidaoui, M. S., & Davidson, M. (2013). Experimental verification of the kinetic differential pressure method for flow measurements. *Journal of Hydraulic Research*, *51*, 634–644. doi:10.1080/00221686.2013.818583

Koutnik, J., & Pulpitel, L. (1996). Modeling of the Francis turbine full-load surge. *Proceedings of the Modeling, Testing and Monitoring for Hydro Power Plants*, Lausanne, Switzerland, *3*, 143–154.

Müller, A., Dreyer, M., Andreini, N., & Avellan, F. (2013). Draft tube discharge fluctuation during self-sustained pressure surge: Fluorescent particle image velocimetry in two-phase flow. *Experiments in Fluids*, *54*, Art. No. 1514. doi:10.1007/s00348-013-1514-6.

Ng, S. L., & Brennen, C. (1978). Experiments on the dynamic behavior of cavitating pumps. *Journal of Fluids Engineering*, *100*, 166–176.

Philibert, R., & Couston, M. (1998). Francis turbine at part load: Matrix simulating the gaseous rope. *Proceedings of the 19th IAHR Symposium on Hydraulic Machinery and Systems*, *Singapore, 1*, 441–453.

Rubin, S. (2004). An interpretation of transfer function data for a cavitating pump. *Proceedings of the 40th AIAA Joint Propulsion Conference*, Florida, United States, AIAA-2004-4025.

Stirnemann, A., Eberl, J., Bolleter, U., & Pace, S. (1987). Experimental determination of the dynamic transfer matrix for a pump. *Journal of Fluids Engineering*, *109*, 218–225.

Streeter, V. L., & Wylie, E. B. (1967). *Hydraulic transients*, New York: McGraw-Hill.

Tsujimoto, Y., Kamijo, K., & Brennen, C. E. (2001). Unified treatment of flow instabilities of turbomachines. *Journal of Propulsion and Power*, *17*, 636–643.

Washio, S., Takahashi, S., & Yamaguchi, S. (1996). Measurement of transiently changing flow rates in oil hydraulic column separation. *JSME International Journal, Series B: Fluids and Thermal Engineering*, *39*, 51–56.

Washio, S., Takahashi, S., Yu, Y., & Yamaguchi, S. (1996). Study of unsteady orifice flow characteristics in hydraulic oil lines. *Journal of Fluids Engineering*, *118*, 743–748.